



Studies of Urban Safety Improvement for Anti-Corrosion Smokestack Protection Based on LOP Strategies

ZHEN TIAN and HUAICHEN HU, School of Mechanical and Automotive Engineering, South China University of Technology, Guangdong, China

With the continuous expansion of urban industry, there is a great risk of fire and explosion during the application of anti-corrosion protection in smokestacks construction. The safety improvement was proposed using **Computational Fluid Dynamics (CFD)** simulation including process design and comprehensive protective approach based on **Layers of Protection (LOP)** strategies. The safety of construction was improved by the development of flammable gas monitoring and an alarming ventilation control system widely used in urban regulatory network. The concentration of flammable gas in the hanging basket is controlled below 5.0% of the lower explosion limit with the possibility to reduce this further to as low as 1.0%. The threat of smokestacks explosion to urban safety is greatly reduced. This system has a certain reference value for the government and factories to use digital tools to improve construction efficiency and urban safety.

CCS Concepts: • **Social and professional topics** → *Professional topics*;

Additional Key Words and Phrases: Urban safety, smokestack anti-corrosion engineering, LOP strategies, numerical simulation

ACM Reference format:

Zhen Tian and Huaichen Hu. 2022. Studies of Urban Safety Improvement for Anti-Corrosion Smokestack Protection Based on LOP Strategies. *Digit. Gov.: Res. Pract.* 3, 4, Article 25 (December 2022), 13 pages.
<https://doi.org/10.1145/3528622>

1 INTRODUCTION

With the continuous development of urbanization, China is promoting modernizing its national governance system and governance capacity. Digital network technology is widely used in traffic management, economic activities and public health services, bringing convenience and comfort to urban residents [1, 2]. In urban safety governance, real-time and accurate digital monitoring networks established by the government can play a preventive and protective role in response to natural disasters such as floods, typhoons, and earthquakes [3]. However, in concern of dealing with the threat of urban industry to safety, there is little attention on the application of urban regulatory network. The traditional regulation mostly depends on manpower, which is in a very inefficient mode [4]. For example, once an accident occurs in the chemical industry, it is very easy to bring multiple negative effects such as safety and economy to the city.

The financial support of Special Funds for Production Safety in Guangdong Province, P. R. China is greatly appreciated.

Authors' address: Z. Tian (corresponding author) and H. Hu, School of Mechanical and Automotive Engineering, South China University of Technology, No. 381 Wushan Road, Tianhe District, Guangdong 510641, China; emails: zhentian@scut.edu.cn, sc6879526@163.com.

Permission to make digital or hard copies of all or part of this work for personal or classroom use is granted without fee provided that copies are not made or distributed for profit or commercial advantage and that copies bear this notice and the full citation on the first page. Copyrights for components of this work owned by others than ACM must be honored. Abstracting with credit is permitted. To copy otherwise, or republish, to post on servers or to redistribute to lists, requires prior specific permission and/or a fee. Request permissions from permissions@acm.org.

© 2022 Association for Computing Machinery.

2639-0175/2022/12-ART25 \$15.00

<https://doi.org/10.1145/3528622>

Digital Government: Research and Practice, Vol. 3, No. 4, Article 25. Publication date: December 2022.

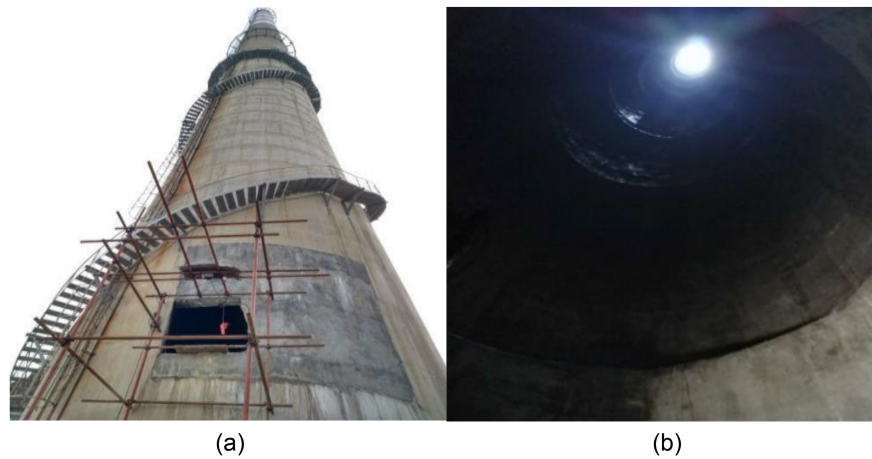


Fig. 1. Exterior (a) and interior (b) appearance of smokestack construction scene.

Wet desulfurization of flue gas using limestone and gypsum is a mature and widely used technology in the city plants to reduce more than 95% sulfide emission in flue gas. Therefore, the maintenance and management of smokestacks plays a very important role in urban safety and environmental protection. Since the flue gas easily forms strongly corrosive mixed solutions of dilute sulfuric acid, inner walls of smokestacks must be protected against corrosion. Constructing the anti-corrosion protection at the inner walls of smokestacks is a space-limited and time-consuming operation with poor air circulation, obstructed vision, and with dangers of poisoning and workers falling from heights [5, 6]. When anti-corrosive coatings are used in construction, flammable gases mixed with air accumulate locally in the working area of smokestacks situating fire and explosion accidents. For the government, it is difficult to supervise these risks through traditional means. It is very necessary to adopt optimized design of the construction process to make more effective use of digital technology and networks supervising urban safety. This research supported by Guangdong Province is conducted based on an investigation of an explosion in a smokestack. The smokestack anti-corrosion construction scene is shown in Figure 1.

During the construction of the anti-corrosion project in 2017 at a 120-meter smokestack of a paper mill in Guangdong province, P. R. China, the use of anti-corrosive paint resulted in volatile flammable vapors accumulated at the working platform – the high-altitude hanging basket inside the smokestack. An electric spark caused a flash fire igniting a large-area fire over the wall surface. The smokestack effect caused the high-temperature gas moving up quickly burning through the hawser of the hanging basket at the top of the smokestack. As a result, the hanging basket fell to the ground killing six workers and causing direct economic losses of about 14 million yuan. Similar fire accidents often happen in the heating and power plants when anti-corrosion measures are applied to desulfurization towers.

Safety systems can be generally categorized as preventive/protective systems or active/passive systems. The protective system reduces the adverse effects of the event. This means that an event is contained or controlled, protecting the equipment from being severely damaged or destroyed. Preventive systems, depending on the design purpose, eliminate (sometimes reduce) the possibility for occurrence of an unexpected event, like an explosion, therefore this approach is always the most highly recommended. The **Layers of Protection (LOP)** shown in Figure 2 is also recognized as **Independent Protection Layers (IPLs)** [7]. The activation sequence is set according to the propagation of an accident. The inner layer will take place first as it is the most effective strategy [8].

In this research, the safety strategies are assigned to be three modules: elimination of combustion necessary factors, monitoring and alarming system, protection and emergency response. And an eddy diffusion model

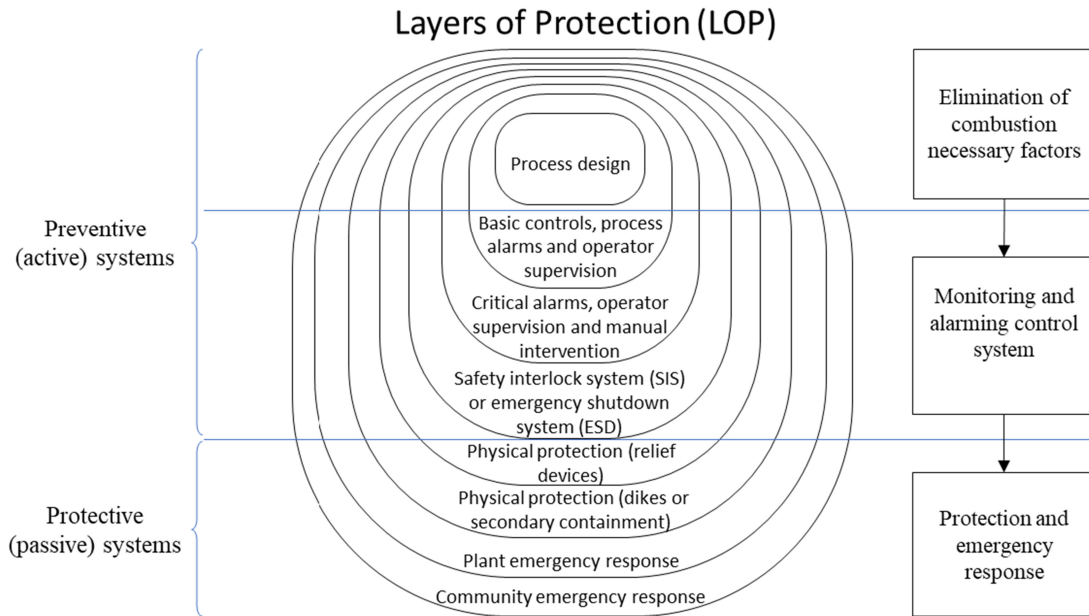


Fig. 2. LOP strategies.

of flammable gas volatilization proposed by Hansen et al. [9] was applied to the simulation on anti-corrosion construction. Then practical suggestions improving urban safety are proposed for the government based on LOP strategies and digital technology.

2 SIMULATION OF FLAMMABLE GAS VOLATILIZATION

2.1 Composition of Flammable Volatile Gases

The working conditions at the application of anti-corrosion coating, glass flake mastic in a smokestack, are shown in Figure 3. The volatile flammable component of the mastic is styrene, providing the major concern as a burning substance when applied inside the smokestack at a large area [10]. Thinner water is commonly known as banana water, one of the main components of paint solvent thinner. It is mainly composed of xylene, n-butyl acetate, ethyl acetate, n-butanol, and acetone. The gas volatilizing from the outermost layer of the coating contains more than 90% relatively heavy xylene (molar mass $106.17 \text{ g mol}^{-1}$), providing flammable volatile compounds diffused to the air, easily accumulating in dangerous concentrations near the hanging basket.

To reduce the complexity of the model, the flammable gas at the construction site was replaced with xylene assuming its instant evaporation at a constant rate of coating.

2.2 Modeling of the Air Movement in the Smokestack

Airflow in smokestacks is usually characterized as turbulent [11]. Tauseef et al. [12] used several turbulence models in CFD describing the eddy diffusion of flammable or toxic heavy gases in the presence of obstacles. The modeling results were compared with the heavy gas diffusion experiments conducted by **Health and Safety Executive (HSE)**, UK, demonstrating spatial and temporal distributions of gas concentrations fitting the best way to the experimental data when using the realizable $k-\epsilon$ model [12–14]. A realizable $k-\epsilon$ turbulence model and a mixed component transport model were used to simulate smokestack corrosion.



Fig. 3. Working conditions at the bottom platform of the smokestack (a) and hanging basket (b) at an application site of anti-corrosion glass flake mastic coating.

2.2.1 Governing Equations. The fundamental equations governing the motion of steady turbulent flows without body forces are the time-averaged Navier-Stokes and continuity equations [15]. For an incompressible flow, they can be written as:

Continuity equation:

$$\frac{\partial U_i}{\partial x_i} = 0 \quad (1)$$

Momentum equation:

$$U_j \frac{\partial U_i}{\partial x_j} = \frac{1}{\rho} \frac{\partial}{\partial x_j} (-P \delta_{ij} + 2\nu S_{ij} - \overline{u_i u_j}) \quad (2)$$

Where ρ is the density of fluid, kg m^{-3} ; ν the kinematic viscosity, $\text{m}^2 \text{s}^{-1}$; P the mean pressure, $\text{kg m}^{-1} \text{s}^{-2}$; S_{ij} is the velocity strain rate tensor expressed as $S_{ij} = 1/2 (\partial U_i / \partial x_j + \partial U_j / \partial x_i)$ and δ_{ij} is the Kronecker delta. U_i and u_i represent the mean and fluctuating velocity components, m s^{-1} ; respectively.

The Reynolds stress terms $-\overline{u_i u_j}$ represent the diffusive transport of momentum by turbulent motion. For the realizable k- ϵ model, turbulent Reynolds stresses and mean velocity gradients were related by turbulent viscosity using the Boussinesq assumption. The mathematical expression for this is:

$$-\overline{u_i u_j} = \nu_t \left(\frac{\partial U_i}{\partial x_j} + \frac{\partial U_j}{\partial x_i} \right) - \frac{2}{3} k \delta_{ij} \quad (3)$$

Turbulent kinetic energy k and turbulent dissipation rate ϵ characterizing the local state of turbulence are related to the turbulent viscosity in the so-called “two equations” model by the following equation:

$$\nu_t = C_\mu \frac{k^2}{\epsilon} \quad (4)$$

where C_μ is a parameter that depends upon the turbulence model; turbulent kinetic energy, k , is written as:

$$k = \frac{1}{2} \overline{u_i^2} \quad (5)$$

with $\overline{u_i^2}$ representing the Reynolds normal stresses, $\text{m}^2 \text{s}^{-2}$.

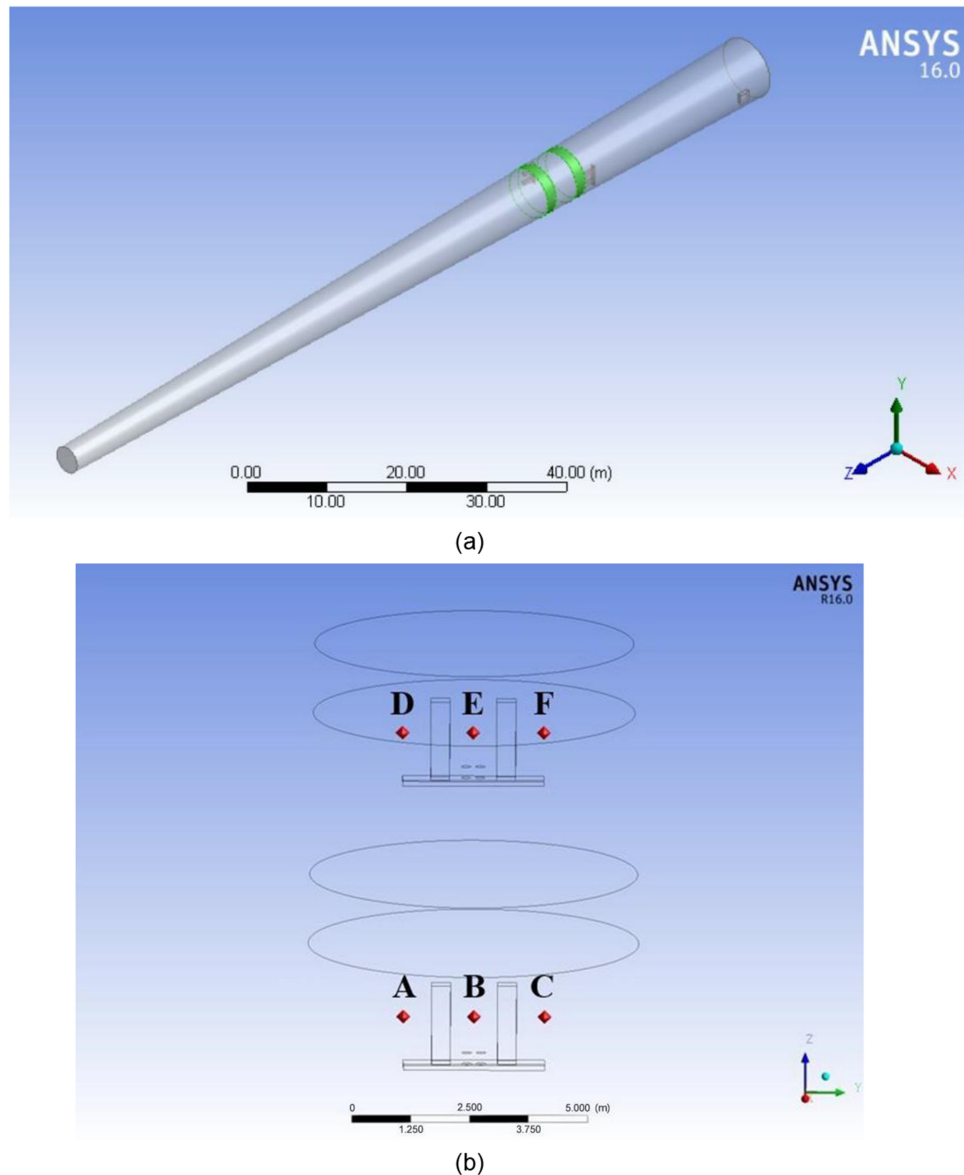


Fig. 4. A smokestack model rendering (a) and xylene concentrations monitoring points (b).

2.2.2 Model Description. The finite element analysis software FLUENT was used to mesh the calculation area in the smokestack. The number of Nodes is 816,299 and the total number of grids is 560,520. To improve the calculation accuracy, the smokestack's external air inlet, the surface of volatile flammable gas, i.e., inner wall coating surface, were grid encrypted. The average mesh quality has exceeded the empirical value of 0.7 [16–18]. The detailed design of the geometric model is shown in Figure 4.

Since the power distribution box with its switches prone to electric spark discharges is positioned at a height of about 1 m in the middle of the basket, six points were selected for the xylene concentration monitoring at the coordinates shown in Table 1.

Table 1. Coordinates of Xylene Concentrations Monitoring Points

| Hanging Basket | Monitoring point | Coordinates, m | | |
|--------------------|------------------|----------------|------|----|
| | | x | y | z |
| Lower basket No. 2 | A | 2.8 | -1.5 | 31 |
| | B | 2.8 | 0 | 31 |
| | C | 2.8 | 1.5 | 31 |
| | D | -2.7 | -1.5 | 36 |
| Upper basket No. 1 | E | -2.7 | 0 | 36 |
| | F | -2.7 | 1.5 | 36 |

2.3 Preliminary Model Verification

The local wind velocities obtained from the field investigation range from 2 to 8 m s⁻¹. The wind velocity as a model parameter was set to 5 m s⁻¹, which was the value of the day of the accident, and also the average value of local wind velocities. At the same time, the xylene gas concentration meter is used to measure in the smokestack. The duration of the experiment is the same as that of the simulation setting, which is 60 minutes, and the time interval is one minute. The xylene concentrations at the monitoring points obtained by simulation were compared with the experimental measurements showing the average relative deviation not exceeding 3.0%.

3 RESULTS AND DISCUSSION

3.1 Analysis of Xylene Accumulation in the Smokestack

The velocity vector of the flow field in the inner space of the smokestack in 60 minutes of simulated xylene volatilization is shown in Figure 5. The outside air enters the smokestack from its bottom inlet colliding with the inner wall. Since the inner diameter of the smokestack gradually decreases with height, the upward velocity of the gas increases at the constant volumetric flow rate providing the exit velocity of about 1 m s⁻¹.

The turbulence developed in the smokestack channel, however, seriously attenuates the energy of the airflow reducing its average velocity. The lower hanging basket was placed to the area of low velocity at the wider cross-section of the smokestack. The airflow additionally tribalized when colliding with the upper hanging basket at a certain height demonstrates additional attenuation of the velocity. Low air velocity at about 0.6 m s⁻¹ near both baskets makes xylene vapors locally accumulate around both hanging baskets [19].

The actual effects of turbulence reduced airflow velocity, and local obstacles (hanging baskets) on the volatilization and eddy diffusion of the flammable xylene in the smokestack was analyzed at variable wind inlet velocity using the CFD numerical simulation method [10, 12].

3.2 Simulation Analysis of the Effect of Wind Velocity on Flammable Xylene Concentration

Figure 6 shows the trend of xylene concentration variation during the anti-corrosion coating construction at each monitoring point at wind velocities of 2, 5, and 8 m s⁻¹ at the smokestack's bottom inlet. One can see that the concentration of xylene in the baskets decreased with increasing air velocity indicating the dilution effect on xylene.

3.3 Simulation of Flammable Xylene Volatilization and Eddy Diffusion in Conditions of Enhanced Ventilation

Explosion prevention systems can be described as inerting (oxidizer concentration control), flammable concentration control, and ignition source avoidance. However, in this case, the flammable gas mixture is present in a process that cannot be fully enclosed, thus inerting is precluded.

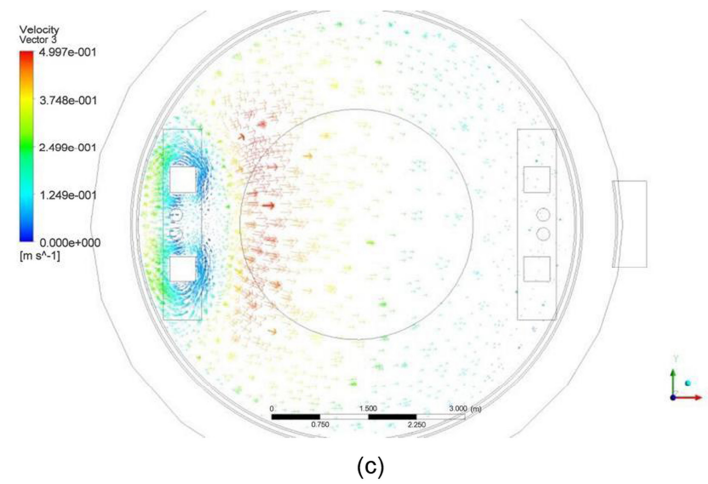
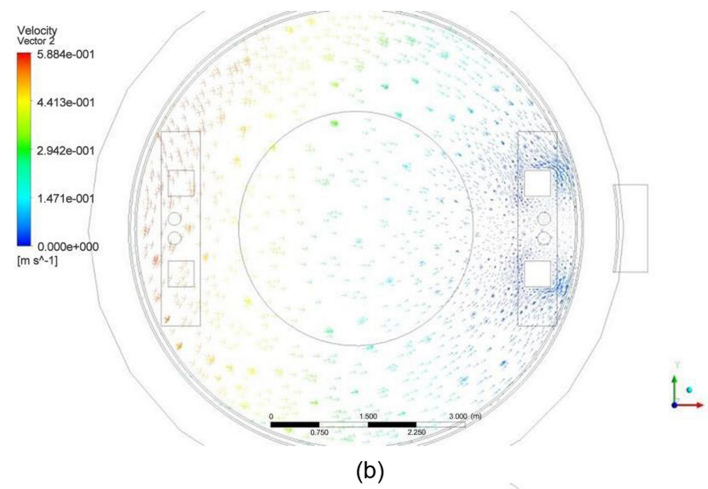
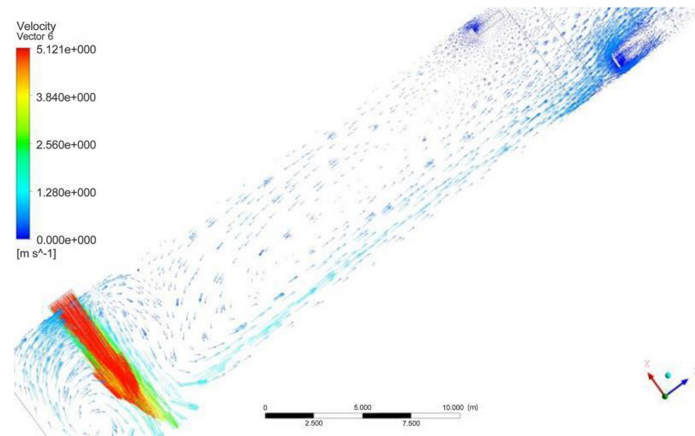


Fig. 5. Velocity vector diagram in the smokestack internal flow field at $y = 0$ m (a) $z = 31$ m (b) and $z = 36$ m (c).

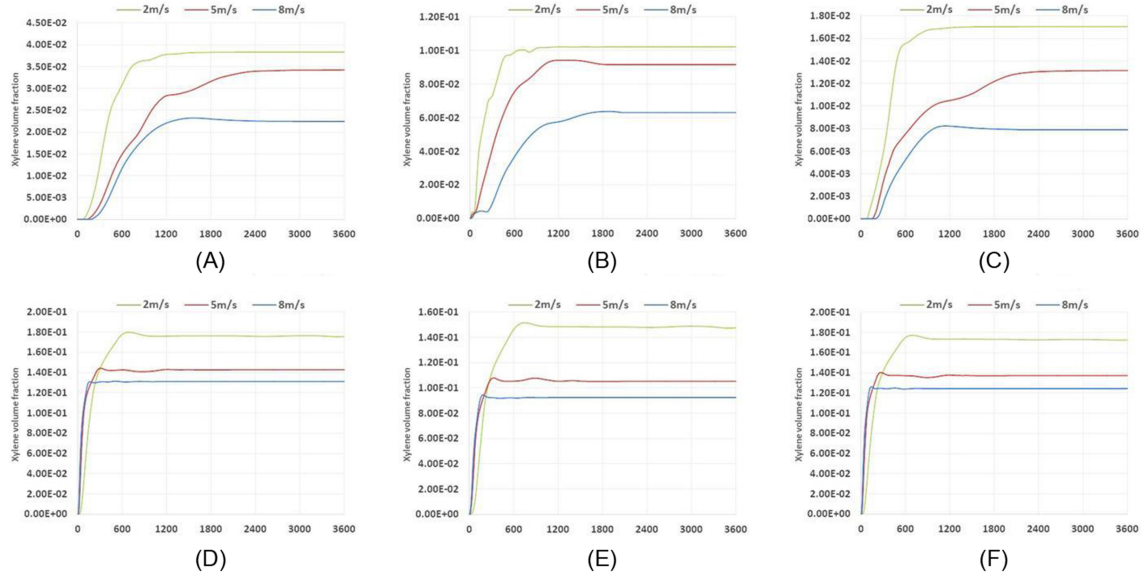


Fig. 6. Xylene concentrations at monitoring points in the smokestack with different inlet airflow velocities.

In the mature digital management of the mining industry, ventilation is a common strategy preventing the gas concentration from entering the explosive range, i.e., ensuring that the gas concentration remains below the **lower explosion limit (LEL)** by means of automatic monitoring and control. Ventilation parameters in an actual case and solutions for gas hazards and fire risks in a coal mine were researched by Cheng et al. [20]. Jiao et al. [21] studied the layouts of dilution ventilation through CFD simulation to examine and compare their effectiveness. Thus, a new solution was proposed in the research: based on the digital smokestack model, baskets were equipped with fans accelerating xylene vapors dilution with air at the coating application area. Fan's capacity required for safe vapors dilution was calculated using Equation (6):

$$L = \frac{M}{C_1 - C_0} \quad (6)$$

Where L is the fan capacity, $\text{m}^3 \text{h}^{-1}$; M - the emission of flammable vapors, $\text{m}^3 \text{h}^{-1}$; C_1 - the lower flammable vapor concentration limit, vol. %; C_0 - concentration of flammable vapor in the supplied air, vol. %.

The emission of flammable vapors can be obtained from the simulation results. Referring to the safe limits of flammable gas concentrations in limited space given in GB 12942-2006, National Standard of P. R. China, the upper limit of xylene concentration in the hanging basket should not exceed 0.05 vol. %. thus, making the minimum fan capacity of about $1,400 \text{ m}^3 \text{h}^{-1}$.

Simplifying the model, the airflow provided by the centrifugal fan is set as an air duct with a square cross-section sized $0.5 \times 0.5 \text{ m}^2$. The average wind velocity in such air duct was calculated using Equation (7):

$$V = \frac{L}{3600F} \quad (7)$$

Where V is the average wind velocity, m s^{-1} , F - ventilation area of vent, m^2 .

The resultant average velocity of air at the outlet of the fan of chosen capacity comprised about 1.6 m s^{-1} . The fan mounted at the guardrail of the rear side of the hanging basket (far side from the wall of the smokestack) at the height about 0.7 m from the basket floor blows to the wall across the basket. The simulation results (Figure 7) show the fan-driven upward eddy diffusion of xylene vapors in the vertical direction (a), and, in the horizontal

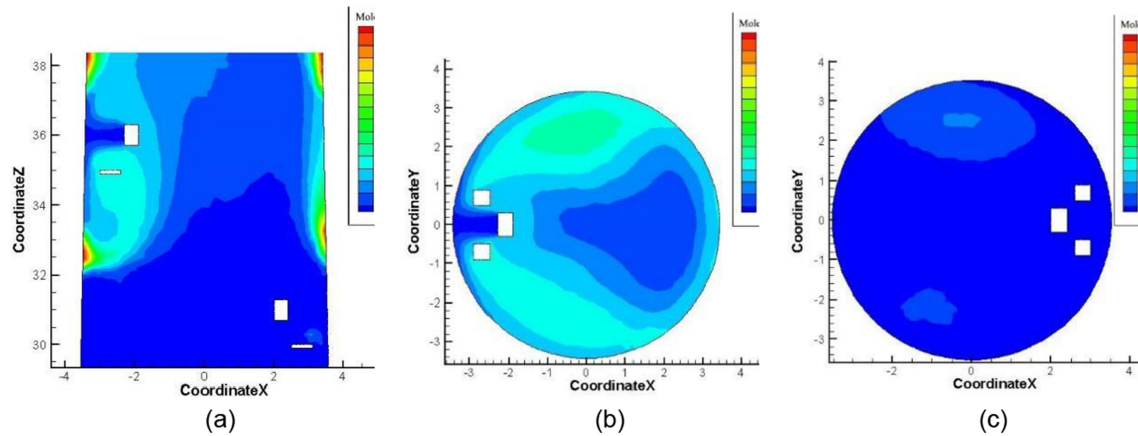


Fig. 7. Distribution of xylene vapor concentration in smokestack sections in 60 min of anti-corrosion coating application: vertical cross-section at $y = 0$ (a),/cross-section at $z = 36$ m (b) and $z = 31$ m (c).

cross-section (b and c), xylene vapors are distributed outside the basket mainly due to the ventilation wind of the fan.

Observations at the monitoring points showed xylene concentrations in the middle of the upper hanging basket No. 1 (Figure 7(b)) being reduced to the desired 0.05% vol. after the fan installation.

The xylene concentration field of the lower hanging basket No. 2 (Figure 7(c)) in the simulated conditions was determined by the amount of accumulation being quite low: the xylene concentration in the smokestack obviously decreased as a result of ventilation reducing the background xylene concentration to around 0.03% vol.

Therefore, a fan with proper capacity installed at the hanging basket appeared to be effective in reducing xylene concentration at both hanging baskets below the risk of ignition.

4 IMPROVEMENT BASED ON LOP STRATEGIES

Based on the simplified LOP strategies introduced above, improvement of the smokestack anti-corrosion construction is discussed targeting elimination or reduction of the fire and explosion risks.

4.1 Elimination of Combustion Necessary Factors

4.1.1 Electrical Safety in Ignition Prevention Design. Sparking safety. Fans, electric mixers, power distribution boxes, LED lighting, electric sockets, and other electric equipment must meet the requirements of ExdIIAT1 explosion-proof grade design.

Static electricity safety. The metal casing of hanging baskets must be reliably grounded at the grounding resistance not exceeding 4.0Ω with clearly visible grounding marks at the grounded device. The insulation resistance between the live element and the basket body must exceed $2.0 \text{ M}\Omega$.

Electric shock safety. The power distribution box and other equipment used in the hanging baskets should belong to the three-level distribution two-level protection system equipped with overheating, short-circuit, and leakage protection devices. Waterproof design must be applied.

4.1.2 Mechanical Ventilation Equipment. To reduce vibration and noise generated by the fan together, fans may be installed on the top of the smokestack aspirating the xylene vapors through an allocated pipe away from the hanging basket for better use of the smokestack effect. Fresh air supplied through the bottom inlet of the smokestack provides continuous ventilation of all the volume [22].

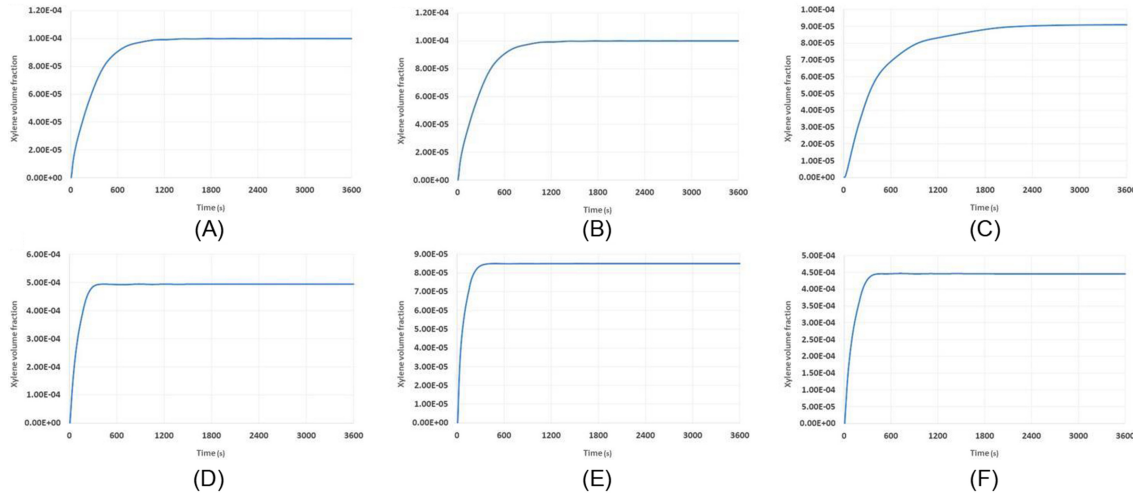


Fig. 8. Xylene concentration in monitoring points varied with coating application time with the installed exhaust fan.

Since centrifugal fans provide higher wind pressure than axial fans of comparable power, the centrifugal exhaust fan of a 4-72 model (consumed power 5 kW at the full pressure of 1500 Pa) was centrally positioned at the top of the smokestack providing maximum airflow of $6,800 \text{ m}^3 \text{ h}^{-1}$. To avoid uncomfortable excessive wind velocity in the smokestack disturbing the workers' operation, an adjusting ventilation pipe is installed at the fan air outlet to control the wind velocity in the working area slightly below Grade 2 according to GB/T 28591-2012, National Standard of P. R. China. The wind velocity at the fan outlet is set at 3 m s^{-1} providing the lowest xylene concentration in the hanging baskets at about 1% of the lower limit of explosion. Equation (7) was used to calculate the cross-section area of the vent giving the ventilation pipe diameter of 0.96 m rounded to 1.0 m [23]. The modeling with boundary conditions adjusted in accordance with the new installed ventilation equipment showed concentrations of xylene in monitoring points of hanging baskets (Figure 8). One can see that the concentration of xylene in upper and lower hanging baskets does not exceed 5% of its lower explosion limit, thus eliminating the risk of ignition.

4.2 Monitoring and Alarming Control System.

4.2.1 Monitoring and Alarming Device for Flammable Vapors Concentration. Real-time monitoring of xylene concentration and alarm-setting equipment must be installed in the hanging baskets [24]. Since the accident scene investigation showed the electric sparks generated in the switches and sockets of power supply and distribution box, the xylene concentration sensors should be installed at the walls and the bottom of the distribution box [25].

4.2.2 Equipment Linkage Setting. For efficient use of safety equipment described above, the fan should be combined with the monitoring and alarm-setting of the xylene vapor concentration in a linked xylene monitoring and alarming ventilation control system (Figure 9). Such a system provides intelligently customized ventilation combining safety and energy savings: having xylene concentration of 0.05% vol. as a benchmark, the fan either stands idle or automatically starts strengthening the ventilation in the smokestack, stopping when the concentration of xylene drops down to 0.01% vol. If accidentally the fan did not start automatically when the xylene concentration reaches the limit of 0.05% vol., the audible and visual warning signals are generated to urge the personnel immediately to start the fan manually. If the manual start fails, the fault signal will be informed to the management personnel through the emergency network. The data recorded by the system will be used to

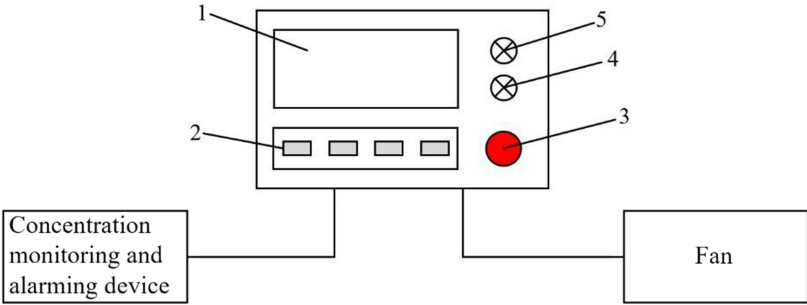


Fig. 9. Schematic outline of linked xylene monitoring and alarming ventilation control system: 1 – display screen; 2 – control buttons (fan on/off, calibration, query, return); 3 – system on/off button; 4 – automatic indicator lamp; 5 – manual indicator lamp.

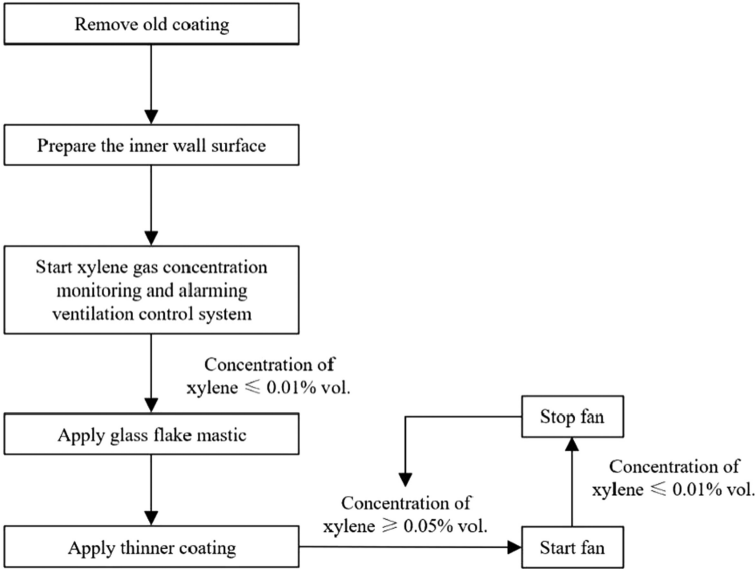


Fig. 10. Improvement process route of anti-corrosion coating application process in a smokestack.

analyze and handle faults, and the workers are evacuated to a safe place until the problem is solved. When an accident occurs, government departments can also conduct evacuation and rescue according to this information. The safety of anti-corrosion coating application can be improved in accordance with the LOP strategies. The related process route is depicted as shown in Figure 10.

4.3 Protection and Emergency Response

4.3.1 Ensuring the Safety of Cross Operation. The application of anti-corrosion coating in smokestacks shall not be carried out simultaneously with other work at height. In the process of anti-corrosion construction, it is necessary to avoid the occurrence of vertical cross of different working surfaces as far as possible, to prevent the falling of materials, tools and other objects from hitting and injuring. If cross operation cannot be avoided, corresponding cross operation risk identification must be conducted before operation, and safety measures should be taken to avoid accidents. The operation area should be isolated and guarded to prevent irrelevant personnel from entering.

4.3.2 Safety Accessories for Protection. To prevent the burn-through and breaking of the hanging basket hawser in the fire with subsequent falling from heights, the hawser should be selected as fire- and high-temperature resistant made of heat-resistant steel. Safety helmets, belts and other safety equipment must be provided to workers. The fire-fighting equipment including fire extinguishers and fire breathing equipment should be ready for fire accidents.

4.3.3 Evacuation and Rescue. Emergency response is a systematic project, involving personnel arrangement, rescue equipment, evacuation plan and response mode. Evacuation drills and rescue training should be carried out frequently to ensure timely evacuation and rapid rescue and reduce negative losses to the greatest extent.

4.3.4 Comprehensive Application in Urban Supervision Network. According to the latest data released by the Department of Ecology Environment of Guangdong Province, in 2020, the average annual concentration of sulfur dioxide in 21 prefecture-level cities in Guangdong Province is $8 \mu\text{g m}^{-3}$. Acid rain occurred in 15 cities and 8 cities were polluted by acid rain. At present, desulfurization technology still plays an important role in controlling sulfur dioxide emissions, and there are more than 2,500 factories that emit flammable and polluting gas, therefore it is of great significance to supervise the smokestacks of these enterprises. By the connection between the monitoring system and the urban supervision network, the government can not only obtain reliable information in the shortest time, but also further use data analysis technology to dispatch rescue materials and personnel, investigate and obtain evidence of accident causes, count casualties and property losses, and the planning and design of reconstruction. Thus, the government can quickly respond to emergencies and improve the capacity of urban security governance.

5 CONCLUSIONS

Based on the concept of digital management, a smokestack anti-corrosion coating application project was analyzed using the CFD simulation method. The numerical simulation showed enhanced ventilation being effective in controlling the flammable vapor concentration in hanging baskets near the potential spark sources below the lower limit of ignition or explosion. Therefore, a flammable gas monitoring and alarming ventilation control system is introduced to the smokestacks' anti-corrosion construction, the collected data can be used to further optimize the construction behavior of workers. The system connected to the emergency management networks will also be more conducive to government managers' decision-making in the prevention and disposal of urban risks.

It is undeniable that the construction of this system requires the government to invest substantial human and financial resources. The management requires the joint participation of multiple departments and the support and feedback from enterprises and citizens. Meanwhile, it is also very important for the government to develop appropriate norms and laws. Besides the gas concentration, the risk of ignition remains if safety regulations are violated by personnel using, e.g., open fire at the workplace without permission [26, 27]. Thus, how to make better use of digital technology to regulate people's behavior affecting industrial safety also should be taken into further consideration.

REFERENCES

- [1] H. Qiuyang, Y. Yongjian, X. Yuanbo, Y. Funing, Y. Zhilu, and S. Yongxiong. 2021. Citywide road-network traffic monitoring using large-scale mobile signaling data. *Neurocomputing* 444 (2021), 136–146.
- [2] G. Yue, C. Jidong, and L. Zhilin. 2022. Government responsiveness and public acceptance of big-data technology in urban governance: Evidence from China during the COVID-19 pandemic. *Cities* 122 (2020), 103536.
- [3] L. Yongsheng, J. Wenliang, Z. Jingfa, L. Binqun, Y. Rui, and W. Xie. 2021. Sentinel-1 SAR-Based coseismic deformation monitoring service for rapid geodetic imaging of global earthquakes. *Natural Hazards Research* 1, 1 (2021), 11–19.
- [4] T. Montbel, C. Huihui, Z. Wei, and P. Selwyn. 2018. Internet of things (IoT) in high-risk Environment, Health and Safety (EHS) industries: A comprehensive review. *Decision Support Systems* 108 (2018), 79–95.

- [5] D. Bulet-Vienney, Y. Chinniah, A. Bahloul, and B. Roberge. 2015. Design and application of a 5-step risk assessment tool for confined space entries. *Safety Science* 80 (2015), 144–155.
- [6] S. Krakowiak and K. Darowicki. 2018. Degradation of protective coatings in steel smokestacks of flue gas desulfurisation systems. *Progress in Organic Coatings* 117 (2018), 141–145.
- [7] T. Fuchino, Y. Shimada, T. Kitajima, K. Takeda, R. Batres, and Y. Naka. 2011. A business process model for process design that incorporates independent protection layer considerations. *Computer Aided Chemical Engineering*, E. N. Pistikopoulos, M. C. Georgiadis, A. C. Kokossis, Elsevier 29 (2011), 326–330.
- [8] W. Ying So, M. H. Hassim, S. I. Ahmad, and R. Rashid. 2021. Inherent occupational health assessment index for research and development stage of process design process. *Safety and Environmental Protection* 147 (2021), 103–114.
- [9] O. R. Hansen, F. Gavelli, S. G. Davis, and P. Middha. 2013. Equivalent cloud methods used for explosion risk and consequence studies. *Journal of Loss Prevention in the Process Industries* 26, 3 (2013), 511–527.
- [10] M. Siddiqui, S. Jayanti, and T. Swaminathan. 2012. CFD analysis of dense gas dispersion in indoor environment for risk assessment and risk mitigation. *Journal of Hazardous Materials* 209–210 (2012), 177–185.
- [11] S. Houda, R. Belarbi, and N. Zemmouri. 2017. A CFD Comsol model for simulating complex urban flow. *Energy Procedia* 139 (2017), 373–378.
- [12] S. M. Tauseef, D. Rashtchian, and S. A. Abbasi. 2011. CFD-based simulation of dense gas dispersion in presence of obstacles. *Journal of Loss Prevention in the Process Industries* 24, 4 (2011), 371–376.
- [13] B. R. Cormier, R. Qi, G. Yun, Y. Zhang, and M. Sam Mannan. 2009. Application of computational fluid dynamics for LNG vapor dispersion modeling: A study of key parameters. *Journal of Loss Prevention in the Process Industries* 22, 3 (2009), 332–352.
- [14] J. Labovský and L. Jelemenský. 2011. Verification of CFD pollution dispersion modeling based on experimental data. *Journal of Loss Prevention in the Process Industries* 24, 2 (2011), 166–177.
- [15] M. Lateb, C. Masson, T. Stathopoulos, and C. Bédard. 2013. Comparison of various types of k- ϵ models for pollutant emissions around a two-building configuration. *Journal of Wind Engineering and Industrial Aerodynamics* 115 (2013), 9–21.
- [16] R. N. Meroney. 2012. CFD modeling of dense gas cloud dispersion over irregular terrain. *Journal of Wind Engineering and Industrial Aerodynamics* 104–106 (2012), 500–508.
- [17] V. Molkov and V. Shentsov. 2014. Numerical and physical requirements to simulation of gas release and dispersion in an enclosure with one vent. *International Journal of Hydrogen Energy* 39, 25 (2014), 13328–13345.
- [18] C. Toliás, S. G. Giannissi, A. G. Venetsanos, J. Keenan, V. Shentsov, D. Makarov, S. Coldrick, A. Kotchourko, K. Ren, O. Jedicke, D. Melideo, D. Baraldi, S. Slater, A. Duclos, F. Verbeke, and V. Molkov. 2019. Best practice guidelines in numerical simulations and CFD benchmarking for hydrogen safety applications. *International Journal of Hydrogen Energy* 44, 17 (2019), 9050–9062.
- [19] S. Gilham, D. M. Deaves, and P. Woodburn. 2000. Mitigation of dense gas releases within buildings: Validation of CFD modeling. *Journal of Hazardous Materials* 71, 1 (2000), 193–218.
- [20] J. Cheng, S. Li, F. Zhang, C. Zhao, S. Yang, and A. Ghosh. 2016. CFD modelling of ventilation optimization for improving mine safety in longwall working faces. *Journal of Loss Prevention in the Process Industries* 40 (2016), 285–297.
- [21] Z. Jiao, S. Yuan, C. Ji, M. S. Mannan, and Q. Wang. 2019. Optimization of dilution ventilation layout design in confined environments using computational fluid dynamics (CFD). *Journal of Loss Prevention in the Process Industries* 60 (2019), 195–202.
- [22] X. Qi, H. Wang, Y. Liu, and G. Chen. 2019. Flexible alarming mechanism of a general GDS deployment for explosive accidents caused by gas leakage. *Process Safety and Environmental Protection*. 132 (2019), 265–272.
- [23] S. J. Kim, H. J. Sung, S. Wallin, and A. V. Johansson. 2019. Design of the centrifugal fan of a belt-driven starter generator with reduced flow noise. *International Journal of Heat and Fluid Flow* 76 (2019), 72–84.
- [24] D. P. Nolan. 2019. *Chapter 17 - Fire and Gas Detection and Alarm Systems*. D. P. Nolan, Gulf Professional Publishing: 303–329.
- [25] R. Vázquez-Román, C. Díaz-Ovalle, E. Quiroz-Pérez, and M. S. Mannan. 2016. A CFD-based approach for gas detectors allocation. *Journal of Loss Prevention in the Process Industries* 44 (2016), 633–641.
- [26] S. Lind. 2008. Types and sources of fatal and severe non-fatal accidents in industrial maintenance. *International Journal of Industrial Ergonomics* 38, 11 (2008), 927–933.
- [27] S. I. Ahmad, H. Hashim, and M. H. Hassim. 2016. A graphical method for assessing inherent safety during research and development phase of process design. *Journal of Loss Prevention in the Process Industries* 42 (2016), 59–69.

Received November 2021; revised March 2022; accepted March 2022